THE JOURNAL OF PHYSICAL CHEMISTRY B

Article

pubs.acs.org/JPCB

Monodisperse PEGylated Spheres: An Aqueous Colloidal Model System

Jeanette Ulama,[†] Malin Zackrisson Oskolkova,[‡] and Johan Bergenholtz*[,†,‡]

[†]Department of Chemistry and Molecular Biology, University of Gothenburg, SE-41296 Göteborg, Sweden

[‡]Division of Physical Chemistry, Center of Chemistry and Chemical Engineering, Lund University, SE-22100 Lund, Sweden

ABSTRACT: Fluorinated core−shell spheres have been synthesized using a novel semibatch emulsion polymerization protocol employing slow feeding of the initiator. The synthesis results in aqueous dispersions of highly monodisperse spheres bearing a well-defined poly(ethylene glycol) graft (PEGylation). Measurements are consistent with the synthesis achieving a high grafting density that moreover consists of a single PEG layer with the polymer significantly elongated beyond its radius of gyration in bulk. The fluorination of the core of the particles confers a low index of refraction such that the particles can be refractive index matched in water through addition of relatively small amounts of a cosolvent, which enables the use of optical and laser-based methods for studies of concentrated systems. The systems exhibit an extreme stability in NaCl solutions, but attractions among particles can be introduced by addition of other salts, in which case aggregation is shown to be reversible. The PEGylated sphere dispersions are expected to be ideally suited as model systems for studies of the effect of PEG-mediated interactions on, for instance, structure, dynamics, phase behavior, and rheology.

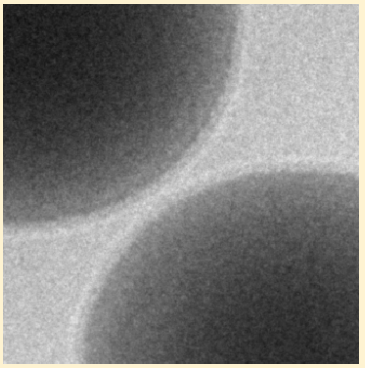

INTRODUCTION

Simple model systems play important roles in science. They provide a proving ground for new concepts and theories and are essential for studying new phenomena in the absence of complicating, extraneous factors. Interparticle attractions between spherical colloidal particles may cause systems to crystallize, glassify, phase separate in two differently concentrated fluids, or undergo aggregation into fractal structures and gels.[1−6] In the pursuit of unraveling the interplay between these, colloid−polymer mixtures, in which added nonadsorbing polymer produces a depletion attraction, have emerged as the model systems of choice.[7] As an alternative, sterically stabilized systems can be used to generate attractions that are controlled to a large extent by the solvent quality for the surface-anchored polymer via mechanisms that are not yet clear.[8] Recent work has come to the conclusion that the degree of solvent penetration in the polymer coat plays an important role for the attraction and that grafted polymers may undergo dramatic structural changes as a function of temperature.[9,10] These studies have been confined so far to nonaqueous systems, and in order to determine the wider applicability of the findings, model systems in aqueous solvents are called for. There are a number of requirements such model systems should fulfill. The particles should be quite monodisperse because even modest amounts of polydispersity can have profound effects on the phase behavior[11] and crystallization kinetics[12] and polydispersity cannot in general be neglected in the analysis of scattering data. Also, since water has a low refractive index, the particles should also possess a similarly low refractive index to enable the use of laser-based methods on concentrated and/or strongly interacting systems. Fluorinated particles are suitable in this regard, and bare, charge-stabilized fluorinated spheres have indeed served well in the past as model aqueous systems for studies of the effect of repulsive interactions on, e.g., translational and rotational dynamics,[13−15] including tracer-particle dynamics,[13,16] phase behavior, and glass transition.[17]

Recently, fluorinated spheres with grafted poly(ethylene glycol), so-called PEGylated particles, were synthesized in an aqueous solvent using emulsion polymerization with the aim of obtaining a model system for fundamental studies.[18] However, these efforts have not yet yielded a successful result in that the polymer graft thickness was observed to far exceed what is expected for a single polymer layer.[18,19] Continued efforts have led to increasingly complex synthesis protocols, which yield multilayered spheres.[20] In the present work, we demonstrate that a simple semibatch emulsion polymerization of methoxy-PEG2000 acrylate macromonomer and heptafluorobutyl methacrylate results in highly monodisperse PEGylated spheres. Semibatch emulsion polymerization is widely used in industry because of its operational flexibility,[21] but it has seen comparatively little use in academia. When applied, it has been the monomer that has been fed to the reaction mixture.[22] The synthesis procedure used in this work employs continuous slow feeding of persulfate initiator solution during the emulsion polymerization. To the best of our knowledge, it is the first time slow feeding of initiator has been used as a route toward monodisperse core−shell spheres. However, we note that Luo and co-workers have previously suggested this and applied it to

Received: January 17, 2014
Revised: February 17, 2014
Published: February 17, 2014

   dx.doi.org/10.1021/jp500568a | J. Phys. Chem. B 2014, 118, 2582−2588

Table 1. Synthesized Batches of Fluorinated Particle Dispersions in Terms of X, the mPEGA/HFBMA Molar Ratio, Amounts of Monomer, Macromonomer, Initiator, Sodium Bisulfite, Stirring Rate, and Resulting Yield along with Hydrodynamic Radius (from DLS) and Polydispersity (from DCP)

batch	X	HFBMA (mL)	mPEGA (g)	$K_2S_2O_8$ (mg)	$NaHSO_3$ (mg)	stirring rate (rpm)	yield (%)	R_H (nm)	$\sigma/\bar{R}$
L0	0	1		11.6	3.8	150	17.2	227	0.055
LS5	0.05	1	0.4998	11.6		50	17.4	92	0.065
L5	0.05	1	0.5010	11.6		150	34.9	101	0.05
LF5	0.05	1	0.5016	11.6		250	60.2	117	0.04
LB5	0.05	1	0.5014	11.6	3.8	150	34.8	130	0.057
L10	0.10	1	0.9998	11.6		150	61.5	114	0.04
L20	0.2	1	2.0008	11.6		150	32.1	98	0.24
L25	0.25	1	2.5000	11.6		150	65.5	41	

emulsion homopolymerization.[23] The rationale for the slow feeding of initiator is to favor propagation by cutting down on radical−radical termination, including PEG−PEG termination, which should lead to improved stability and to narrow size distributions because chains have in this way an equal chance to grow.

The goal of this study is to devise a synthesis route to monodisperse fluorinated spheres with a single, well-defined grafted layer of PEG that imparts stability far superior to that of charge stabilized systems, yet allows for reversible destabilization upon addition of select electrolytes. In what follows, we provide a synthesis protocol that achieves precisely this along with a thorough characterization of the particles and their stability behavior.

EXPERIMENTAL SECTION

Materials. The fluorinated monomer 2,2,3,3,4,4,4-heptafluorobutyl methacrylate (HFBMA, 97%), with a refractive index of 1.342 at the sodium D-lines, was purchased from Alfa Aesar. The inhibitor (hydroquinone) was removed prior to use by passing the monomer through a column packed with material for inhibitor removal (CAS 9003-70-7, Sigma-Aldrich). Dimethylsulfoxide (DMSO, dried, maximum 0.05% water) was purchased from Merck. The initiator, potassium persulfate (KPS), was obtained from Sigma-Aldrich and was recrystallized in water once prior to use. Sodium bisulfite and dodecane (99%), also from Sigma-Aldrich, were used as received. The macromonomer methoxy poly(ethylene glycol) acrylate (mPEGA), with a molecular weight (MW) of 2000 g/mol, was a custom synthesis performed by SunBio (S. Korea) and was used as received. NaCl (99.5%) and Na_2CO_3 (99.9%) were supplied by Merck and were used as received. Colloidal gold particles (NIST) and sucrose (Fluka) were used as received. For purification, dialysis tubes with a cutoff MW of 12−14 kDa from MAKAB were used.

Methods. Dynamic light scattering (DLS) and electrophoresis measurements were performed using a Malvern Zetasizer Nano ZS equipped with a He−Ne laser with a wavelength of 633 nm and a detector positioned at a scattering angle of 173°. The hydrodynamic radius was extracted from a second-order cumulant analysis. The same instrument was used for determination of the zeta (ζ) potential using a folded capillary cell. The zeta potential was determined from Smoluchowski's equation, $u = \epsilon_0\epsilon_r\zeta/\eta$, in which u is the electrophoretic mobility, ϵ_r is the dielectric constant, ϵ_0 is the permittivity of vacuum, and η is the solvent viscosity. It was logged as an average of five consecutive runs. These measurements were done at 25 °C.

Size distributions were obtained by disc centrifugation photosedimentometry (DCP) using a disc centrifuge (CPS Instruments, model DC18000). In this instrument, the sedimentation of the particles proceeds in a density gradient generated by sucrose (8−22 wt %) solutions in an optically clear, rotating disc, which is sealed with dodecane to prevent evaporation. When particles approach the outer edge of the rotating disc, they scatter a portion of a (405 nm wavelength) light beam that is passed through the disc. The decrease in transmitted light intensity is continuously recorded as the sedimenting dispersion passes the detection zone, which is converted into a size-dependent particle concentration by assuming the particles are nonabsorbing homogeneous spherical Mie scatterers. The corresponding particle size is obtained from the sedimentation time taking density and viscosity profiles into account.[24] Colloidal gold particles with a nominal diameter of 60 nm were used to quantify the density gradient. The disc rotation speed was set to either 10000 or 15000 rpm depending on the particle size. Number-average size distributions were extracted from the data from which the polydispersity was calculated as the standard deviation normalized by the mean. The density of the particles was extracted from a linear least-squares slope of the reciprocal dispersion density, measured using a precision density meter (DMA5000, Anton-Paar), as a function of weight fraction. This procedure resulted in particle densities of 1.48 and 1.31 g/mL for latices L5 and L25 (cf. Table 1) at 25 °C. Particle densities of other batches synthesized were obtained by interpolation using these values and 1.59 g/mL, the value for bare, nongrafted particles.[25] The particle density was found to have a negligible effect on the polydispersity determined by DCP.

The refractive index of dispersions was determined by measuring the light transmittance using a Cary Bio 50 UV/vis spectrometer equipped with a Varian PCB 1500 Water Peltier System thermostat for temperature control operating at 25 °C. The measurements were carried out in 10 mm quartz cuvettes for three different wavelengths, 550, 600, and 640 nm. Prior to each new sample, the solvent was measured as a blank. The refractive index of the solvent was varied by adding various amounts of DMSO while maintaining a constant particle concentration.

Samples for cryogenic transmission electron microscopy (cryo-TEM) were prepared in a climate chamber kept at a temperature of 25−28 °C and a relative humidity close to 100% to prevent evaporation from samples during preparation. A 5 μL sample drop was placed on a lacey carbon-coated film supported by a copper grid. Excess sample was removed by blotting with filter paper, leaving a thin (20−400 nm) liquid film in the holes of the carbon film. The grid was subsequently

dx.doi.org/10.1021/jp500568a | J. Phys. Chem. B 2014, 118, 2582−2588

plunged rapidly into liquid ethane at −180 °C and transferred into liquid nitrogen at −196 °C. The vitrified samples were stored in liquid nitrogen and transferred into a Philips CM120 BioTWIN TEM equipped with a postcolumn energy filter (Gatan GIF 100) using an Oxford CT 3500 cryo-holder and its workstation. The acceleration voltage was 120 kV, and the working temperature was kept below −182 °C. The images were recorded digitally with a CCD camera (794IF) under low-dose conditions with an underfocus of less than 1 μm.

SAXS spectra were recorded at the Division of Physical Chemistry, Lund University, Sweden, on an automated SAXS pinhole system (Ganesha, JJ X-ray A/S, Denmark). The instrument is equipped with a high brilliance micofocus sealed tube with shaped multilayer optics and a two-dimensional single photon counting solid-state Pilatus detecor (Dectris Ltd., Switzerland). Data were recorded using a three-pinhole collimation configuration, a sample-to-detector-distance of 1540 mm, and a 2 mm beam-stop, resulting in a scattering vector range of 0.003−0.21 Å^{-1}. Raw data were processed and radially averaged using the SAXSGUI software, and the scattering spectra were obtained as a function of the momentum transfer $q = 4\pi \sin(\theta/2)/\lambda$, where θ is the scattering angle and λ is the wavelength (0.1542 nm, Cu Kα line). The form factor of homogeneous spheres with radii distributed according to a Schulz distribution was used for quantitative analysis. For the large particles examined in this work, the SAXS intensity is strongly affected by instrumental resolution effects originating from the finite size of the beam. To account for this, the model intensity was smeared using a trapezoidal beam profile as done by Wagner et al.,[26] except that the (penumbral) width of the beam was adjusted from the calculated value to agree with a measurement of the unscattered beam.

Synthesis Procedure. In order to determine a suitable range of mPEGA to HFBMA monomer molar ratios, denoted by *X*, four different 100 mL batches have been synthesized. The compositions and corresponding batch labels are given in Table 1. The molar ratio was varied between 0.05 and 0.25 for batches L5−L25, and in addition, a reference batch of particles without mPEGA, labeled L0, was synthesized. The stirring rate during the polymerization was also varied, from 50 to 250 rpm (LS5, L5, and LF5), at fixed *X*. The effect of sodium bisulfite, often used to form a redox pair initiation system with KPS,[27] was also evaluated.

In a typical synthesis, 75 mL of Milli-Q water was added to a three-neck, round-bottom flask and heated to 70 °C by immersion in an oil bath. The water was purged with nitrogen gas to remove oxygen. The stirring rate was set to 500 rpm using an overhead stirrer with a polypropylene blade. The macromonomer mPEGA was dissolved in 25 mL of water, which was added to the reaction vessel followed by 1 mL of the fluorinated HFBMA monomer. The mixture was stirred for 1 h, after which the stirring rate was decreased to 150 rpm when 10 mL of initiator solution (an aqueous solution of KPS and, when present, sodium bisulfite) was added dropwise to the reaction. The duration for the addition of the initiator solution was approximately 3 h. Typically, after about 2 h, a bluish color was observed. To avoid oxygen flow into the reaction vessel and any stripping of the monomer during the initiator addition, a nitrogen gas flow was applied to the reflux condenser, which was monitored with a bubble counter. After roughly 20 h, the batch was left to cool. The dispersion was filtered through 10 μm filter paper twice and through a 1 μm glass syringe filter. All batches were dialyzed against Milli-Q water until the conductivity of the dialyzate was similar to that of the Milli-Q water. This process usually required a few days. After dialysis, the dispersions were filtered through a 0.45 μm filter. In order to prevent bacterial growth during longer-time storage and to obtain a well-defined dispersion medium, NaN_3 and NaCl were added to yield a 10 mM aqueous solution consisting of 7 mM NaCl and 3 mM NaN_3. More concentrated particle dispersions were produced via membrane centrifugal filtration (Jumbosep, Pall, 30 kDa cutoff MW). An estimate of the synthesis yield was obtained by determining the percent dry solids after dialysis and dividing by the total mass percent added in the synthesis less the water.

RESULTS AND DISCUSSION

Generally, it is difficult to produce fluorinated particle dispersions by classical emulsion polymerization.[28] However, aqueous dispersions of sub-micrometer-size fluorinated particles have been generated by single-stage or seeded emulsion polymerization using heptafluorobutyl acrylate[29] and heptafluorobutyl methacrylate[25,30] monomers. Our initial attempts at synthesizing PEGylated poly(heptafluorobutyl methacrylate) (pHFBMA) particles using batch emulsion polymerization, in which the initiator is introduced all at once, were based on a combination of procedures for charge stabilized pHFBMA particles[25] and PEGylated polystyrene spheres.[31] This procedure resulted in dispersions of multimodally distributed particle sizes, which, moreover, exhibited irreversible aggregation at high ionic strength. In contrast, the semibatch approach with dropwise addition of initiator solution subsequently adopted consistently produced highly monodisperse spheres, as seen to some extent in the cryo-TEM image in Figure 1. In addition, the synthesis procedure is robust in that it leads to nearly monodisperse particles for a generous range of molar ratios of the PEG macromonomer to the HFBMA monomer, *X*, as long as it is kept below 0.2. In what follows, we will focus mostly on a molar ratio of 0.05, corresponding to latex L5 in Table 1.

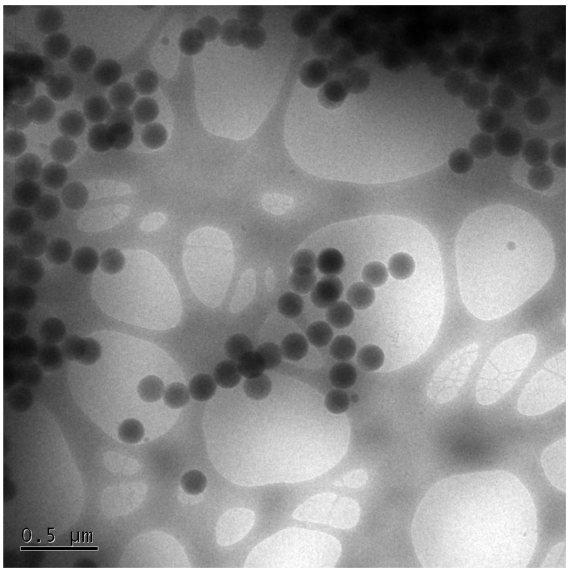

Figure 1. Cryo-TEM image of fluorinated pHFBMA particles bearing grafted PEG of molecular weight 2000, synthesized using a molar ratio of $X = 0.05$ (latex L5).

dx.doi.org/10.1021/jp500568a | J. Phys. Chem. B 2014, 118, 2582−2588

The synthesized particles were characterized regarding size and degree of monodispersity by cryo-TEM, SAXS, and DCP. Figure 2 shows the scattered intensity from a dilute dispersion

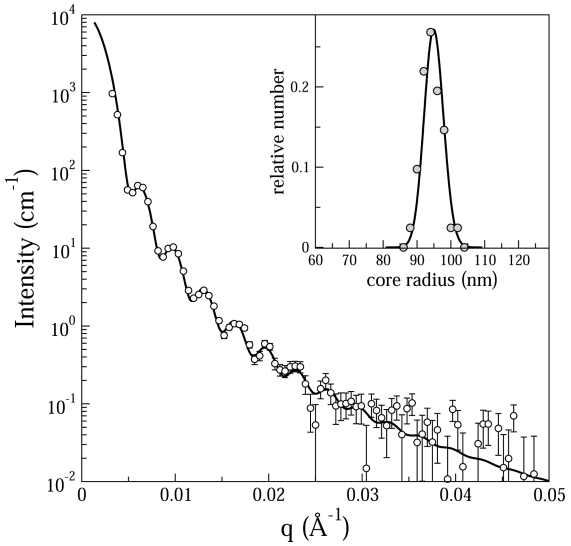

Figure 2. Form factor obtained from SAXS as a function of the wave vector for latex L5. The solid line is a model fit using homogeneous spheres with a mean radius of 95 nm and a 3% polydispersity and taking smearing effects due to beam collimation into account. The inset shows a comparison between the (Schulz) size distribution used in the SAXS analysis (solid line) and a histogram determined from cryo-TEM images (symbols).

of the same particles, as shown in Figure 1. The numerous oscillations as a function of the wave vector indicate that the particles are quite monodisperse. To model the intensity data quantitatively, we neglect the PEGylation and use the form factor for homogeneous spheres with sizes distributed according to a Schulz distribution.[32] This results in excellent agreement with the data in Figure 2 for a mean radius of 95 nm and a polydispersity of just 3%. Furthermore, the size distribution employed in the SAXS modeling is seen to be within 1 nm of the number-based histogram in Figure 2, obtained from cryo-TEM images, from which it is concluded that the solvated PEG graft indeed does not contribute to the SAXS intensity. The polydispersity of the same sample as determined by DCP was 5% (Table 1), a difference that is likely brought about by broadening of the concentration profile by diffusion.

Upon increasing the magnification in the cryo-TEM, the images shown in Figure 3 were recorded, which show bare pHFBMA particles and PEGylated pHFBMA particles near contact. The interparticle contacts are seen to be distinctly different in the two cases. Whereas the nongrafted particles come into direct contact with one another, the PEGylated particles are prevented from doing so by PEG layers which are seen to surround the particles uniformly. The thickness can be estimated from Figure 3 to about 6 nm, which corresponds roughly to 6% of the mean particle radius. Further confirmation of this chain extension comes from comparing the hydrodynamic radius obtained independently by DLS, 101 nm, as reported in Table 1, with the radius of the fluorinated core from the SAXS analysis, which yielded 95 nm. The 6 nm chain extension is about 4 times the unperturbed radius of gyration of PEG2000 in bulk, which has been determined as ≈1.4 nm,[33] and it is roughly 30% of the contour length, estimated to about 20 nm.[34] It follows that the PEG layer is significantly elongated beyond the expected dimension of a mushroom structure, which should be similar to 2 times the radius of gyration.[35] Chain extensions of 6−7 nm have indeed been observed for grafted PEG chains, thought to be in the polymer brush regime, using computer simulations of PEG of essentially the same molecular weight.[36] Thus, our result for the steric layer thickness is consistent with what is expected for a single layer of PEG molecules.

The interactions between the PEGylated particles can be tuned through addition of salt. Electrophoresis measurements of the zeta potential, shown in Figure 4, show that the particles behave as charged spheres at sufficiently low ionic strengths but with lower zeta potentials due to the PEGylation. Similar observations have been made for styrene copolymerized with mPEGA.[31] Note that the zeta potential in Figure 4 is proportional to the electrophoretic mobility. The lower

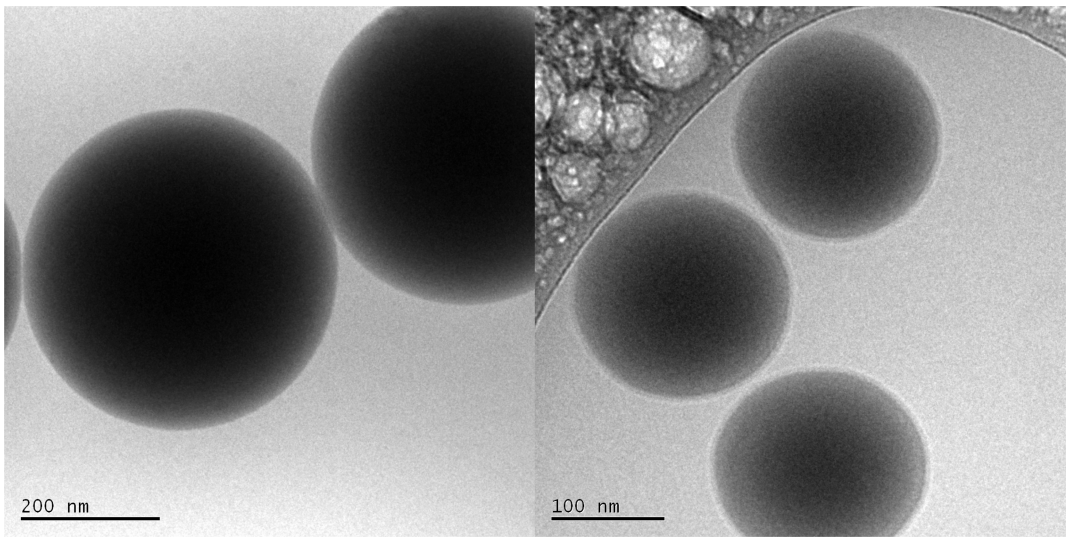

Figure 3. Cryo-TEM images of fluorinated latex beads in contact (left, latex L0) and similarly fluorinated particles bearing surface-grafted PEG (right, latex L5).

dx.doi.org/10.1021/jp500568a | J. Phys. Chem. B 2014, 118, 2582−2588

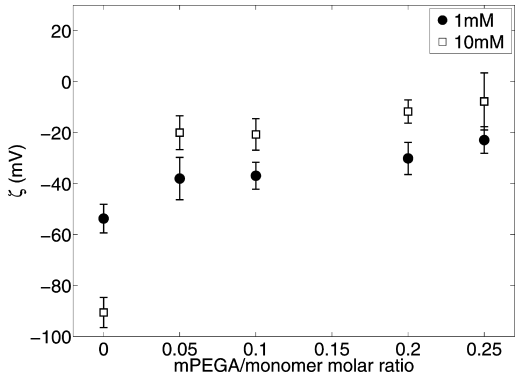

Figure 4. Zeta potential of particles as a function of mPEGA/HFBMA monomer ratio, *X*, dispersed in 1 and 10 mM NaN_3/NaCl solutions, as labeled.

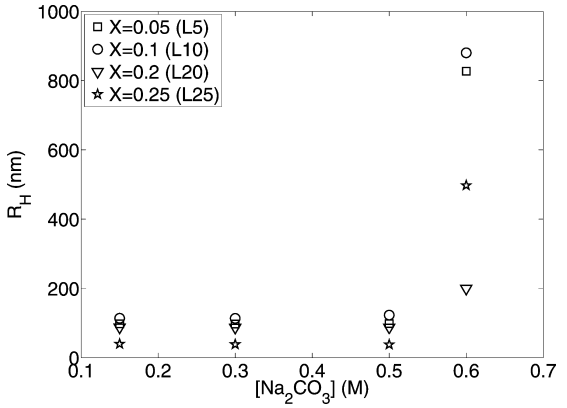

Figure 5. Stability in salt solutions, in terms of apparent hydrodynamic radius as a function of Na_2CO_3 concentration for various mPEGA/HFBMA monomer ratios, *X*, as labeled.

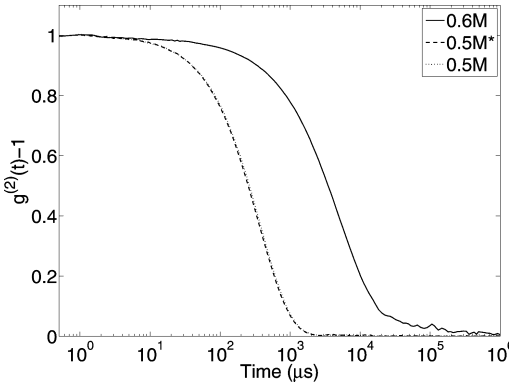

Figure 6. Intensity correlation function versus delay time for the PEGylated spheres in Figure 1 in 0.5 and 0.6 M Na_2CO_3 solutions. * Diluted from 0.6 M Na_2CO_3.

electrophoretic mobility is in line with expectations for charged spheres bearing neutral grafts,[37] which experience increased drag and retardation of the motion of free charges behind the shear plane.[38] From the numerical results of Hill et al.,[38] we infer that for a constant salt concentration and a constant grafted layer thickness the electrophoretic mobility decreases as the overall particle size is decreased. This qualitative trend is in accord with the results in Figure 4, where the L20 and L25 latices exhibit significantly lower zeta potential magnitudes and also smaller particle radii. Furthermore, on increasing the salt concentration from 1 to 10 mM, the zeta potential of the PEGylated particles is lowered, whereas the opposite trend is observed for the bare pHFBMA particles. This behavior is in qualitative accord with observations made by Ottewill and Satgurunathan,[39] and it is also in agreement with predictions of theory.[38] The effect of double layer polarization, which tends to decrease the zeta potential of bare particles as the salt concentration is increased, begins to diminish as the double layer is further compressed by adding salt. This leads to an increasing electrophoretic mobility with increasing salt concentration as observed for the bare pHFBMA particles in Figure 4. Finally, neither the change in stirring rate nor the addition of sodium bisulfite had a significant effect on the zeta potential.

PEGylated particles are typically stable in high-ionic-strength aqueous media. For instance, aggregation of the PEG-covered particles developed by Ferrari et al.[40] was not observed until NaCl concentrations of 4.5 M were reached. The PEGylated particles in this work did not aggregate even in aqueous solutions of 5 M NaCl, which was the highest concentration investigated. As in past work,[41] in order to induce aggregation, Na_2CO_3 was used instead, which is known to cause phase separation in PEG solutions.[42] Particles exhibited long-time stability in 0.5 M solutions of Na_2CO_3, as shown in Figure 5, but aggregated in 0.6 M solutions. Quite crucial for the use as model systems in studies of aggregation and gelation is that, once aggregated, particles can be redispersed. Figure 6 shows an intensity correlation function from DLS for the PEGylated particles dispersed in 0.5 M Na_2CO_3 solution. On increasing the salt concentration to 0.6 M, there is a dramatic shift in the decay time indicative of an aggregated state. Diluting this aggregated system so that it is returned to a salt concentration of 0.5 M results in an intensity correlation function that is indistinguishable from the original one, which shows that a high PEG coverage is achieved in the synthesis.

Due to turbidity in concentrated dispersions, it is often difficult to use optical and light scattering techniques. Refractive index matching solves this problem. In addition, since the van der Waals force depends strongly on the refractive index difference between particles and solvent,[43] this part of the interaction can accordingly be controlled. It is a simple matter to refractive index match these core-solvated shell particles by adding a cosolvent. In Figure 7, the square root of 1 minus the transmittance, which is proportional to the square root of the scattered intensity in the forward direction, is shown as a

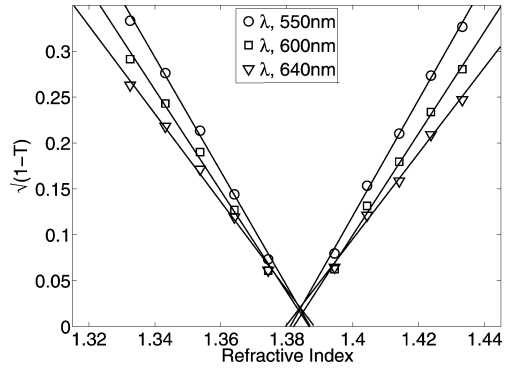

Figure 7. Square root of 1 minus the transmittance as a function of refractive index at three different wavelengths, as labeled.

dx.doi.org/10.1021/jp500568a | *J. Phys. Chem. B* 2014, 118, 2582−2588

function of the refractive index of the solvent. By fitting straight lines to the data near the match point, the lines are found to intersect at a refractive index of 1.384 with no significant dependence on wavelength. This value is between 1.383, the value for bulk pHFBMA,[44] and 1.386, determined for bare pHFBMA particles,[30] which indicates that the solvated PEG layer does not affect the refractive index of the particles significantly.

CONCLUSIONS

A simple semibatch emulsion polymerization procedure has been employed to produce very nearly monodisperse fluorinated spheres with a well-defined PEG graft without the aid of surfactants. The high degree of stability in salt solutions, the PEG layer thickness, and the reversible nature of aggregation suggest that a high grafting density is reached in the synthesis. The low refractive index of the particles, which enables refractive index matching in predominantly aqueous solvents, the near size monodispersity, and the single PEG-layer graft should make the latices useful as model systems in a range of studies.

AUTHOR INFORMATION

Corresponding Author

*E-mail: jbergen@chem.gu.se. Phone: +46 (0)31 786 9078. Fax: +46 (0)31 772 1394.

Notes

The authors declare no competing financial interest.

ACKNOWLEDGMENTS

Financial support from the Swedish Research Council is gratefully acknowledged. The authors thank Gunnel Karlsson (Biomikroskopienheten, Materialkemi, Kemicentrum, Lund University) for her expert help with the cryo-TEM measurements.

REFERENCES

(1) Grant, M. C.; Russel, W. B. Volume-fraction dependence of elastic-moduli and transition-temperatures for colloidal silica. *Phys. Rev. E* **1993**, *47*, 2606−2614.
(2) Verduin, H.; Dhont, J. K. G. Phase-diagram of a model adhesive hard-sphere dispersion. *J. Colloid Interface Sci.* **1995**, *172*, 425−437.
(3) Ilett, S. M.; Orrock, A.; Poon, W. C. K.; Pusey, P. N. Phase behavior of a model colloid-polymer mixture. *Phys. Rev. E* **1995**, *51*, 1344−1352.
(4) Dinsmore, A. D.; Weeks, E. R.; Prasad, V.; Levitt, A. C.; Weitz, D. A. Three-dimensional confocal microscopy of colloids. *Appl. Opt.* **2001**, *40*, 4152−4159.
(5) Pham, K. N.; Puertas, A. M.; Bergenholtz, J.; Egelhaaf, S. U.; Moussaid, A.; Pusey, P. N.; Schofield, A. B.; Cates, M. E.; Fuchs, M.; Poon, W. C. K. Multiple glassy states in a simple model system. *Science* **2002**, *296*, 104−106.
(6) Anderson, V. J.; Lekkerkerker, H. N. W. Insights into phase transition kinetics from colloid science. *Nature* **2002**, *416*, 811−815.
(7) Poon, W. C. K. The physics of a model colloid-polymer mixture. *J. Phys.: Condens. Matter* **2002**, *14*, R859−R880.
(8) Jansen, J. W.; DeKruif, C. G.; Vrij, A. Attractions in sterically stabilized silica dispersions. 3. experiments on phase-separation induced by temperature-variation. *J. Colloid Interface Sci.* **1986**, *114*, 481−491.
(9) Roke, S.; Buitenhuis, J.; van Miltenburg, J. C.; Bonn, M.; van Blaaderen, A. Interface-solvent effects during colloidal phase transitions. *J. Phys.: Condens. Matter* **2005**, *17*, S3469−S3479.
(10) Roke, S.; Berg, O.; Buitenhuis, J.; van Blaaderen, A.; Bonn, M. Surface molecular view of colloidal gelation. *Proc. Natl. Acad. Sci. U.S.A.* **2006**, *103*, 13310−13314.
(11) Liddle, S. M.; Narayanan, T.; Poon, W. C. K. Polydispersity effects in colloid-polymer mixtures. *J. Phys.: Condens. Matter* **2011**, *23*, 194116.
(12) Henderson, S. I.; van Megen, W. Metastability and crystallization in suspensions of mixtures of hard spheres. *Phys. Rev. Lett.* **1998**, *80*, 877−880.
(13) Koenderink, G. H.; Philipse, A. P. Rotational and translational self-diffusion in colloidal sphere suspensions and the applicability of generalized Stokes-Einstein relations. *Langmuir* **2000**, *16*, 5631−5638.
(14) Degiorgio, V.; Piazza, R.; Bellini, T. Static and dynamic light scattering study of fluorinated polymer colloids with a crystalline internal structure. *Adv. Colloid Interface Sci.* **1994**, *48*, 61−91.
(15) Degiorgio, V.; Piazza, R.; Jones, R. B. Rotational diffusion in concentrated colloidal dispersions of hard spheres. *Phys. Rev. E* **1995**, *52*, 2707−2717.
(16) Härtl, W.; Versmold, H.; Zhang-Heider, X. Tracer particle diffusion in crystal- and fluid-like ordered colloidal. *Bunsen-Ges. Phys. Chem., Ber.* **1991**, *95*, 1105−1111.
(17) Härtl, W.; Versmold, H.; Zhang-Heider, X. The glass transition of charged polymer colloids. *J. Chem. Phys.* **1995**, *102*, 6613−6618.
(18) Wiemann, M.; Schneider, R.; Bartsch, E. Synthesis of PEG-Stabilized Fluoro-Acrylate Particles and Study of their Glass Transition in Aqueous Dispersion. *Z. Phys. Chem.* **2012**, *226*, 761−778.
(19) Schneider, R. Synthese und Charakterisierung von Modellkolloiden auf der Basis von PEG-stabilisierten Poly(heptafluorobutylmethacrylat)-Partikeln und Poly(styrol-co-tert-butylmethacrylat)-Mikrogelen. Ph.D. thesis, Albert-Ludwigs-Universität, Freiburg im Breisgau, 2011.
(20) Burger, D.; Gisin, J.; Bartsch, E. Synthesis of sterically stabilized perfluorinated aqueous latices. *Colloids Surf., A* **2014**, *442*, 123−131.
(21) Moore, A. L. *Fluoroelastomers handbook: the definitive user's guide and databook*; William Andrew Publishing: Norwich, NY, 2006.
(22) Chern, C. S. Emulsion polymerization mechanisms and kinetics. *Prog. Polym. Sci.* **2006**, *31*, 443−486.
(23) Luo, Z.; Zou, C.; Syed, S.; Syarbaini, L. A.; Chen, G. Highly monodisperse chemically reactive sub-micrometer particles: polymer colloidal photonic crystals. *Colloid Polym. Sci.* **2012**, *290*, 141−150.
(24) Kamiti, M.; Boldridge, D.; Ndoping, L. M.; Remsen, E. E. Simultaneous absolute determination of particle size and effective density of submicron colloids by disc centrifuge photosedimentometry. *Anal. Chem.* **2012**, *84*, 10526−10530.
(25) Koenderink, G. H.; Sacanna, S.; Pathmamanoharan, C.; Rasa, M.; Philipse, A. P. Preparation and properties of optically transparent aqueous dispersions of monodisperse fluorinated colloids. *Langmuir* **2001**, *17*, 6086−6093.
(26) Wagner, J.; Härtl, W.; Hempelmann, R. Characterization of monodisperse colloidal particles: comparison between SAXS and DLS. *Langmuir* **2000**, *16*, 4080−4085.
(27) Shaffei, K. A.; Ayoub, M. M. H.; Ismail, M. N.; Badran, A. S. Kinetics and polymerization characteristics for some polyvinyl acetate emulsions prepared by different redox pair initiation systems. *Eur. Polym. J.* **1998**, *34*, 553−556.
(28) Landfester, K.; Rothe, R.; Antonietti, M. Convenient synthesis of fluorinated latexes and core-shell structures by miniemulsion polymerization. *Macromolecules* **2002**, *35*, 1658−1662.
(29) Härtl, W.; Zhang-Heider, X. The synthesis of a new class of polymer colloids with a low index of refraction. *J. Colloid Interface Sci.* **1997**, *185*, 398−401.
(30) Pan, G.; Tse, A. S.; Kesavamoorthy, R.; Asher, S. A. Synthesis of highly fluorinated monodisperse colloids for low refractive index crystalline colloidal arrays. *J. Am. Chem. Soc.* **1998**, *120*, 6518−6524.
(31) Brindley, A.; Davis, S. S.; Davies, M. C.; Watts, J. F. Polystyrene colloids with surface-grafted polyethylene oxide as model systems for site-specific drug delivery: I. Preparation and surface chemical characterization using SIMS and XPS. *J. Colloid Interface Sci.* **1995**, *171*, 150−161.

(32) Aragon, S. R.; Pecora, R. Theory of dynamic light scattering from polydisperse systems. *J. Chem. Phys.* **1976**, *64*, 2395−2404.
(33) Rubinson, K. A.; Krueger, S. Poly(ethylene glycol)s 2000−8000 in water may be planar: a small-angle neutron scattering (SANS) structure study. *Polymer* **2009**, *50*, 4852−4858.
(34) Takahashi, Y.; Tadokoro, H. Structural studies of polyethers, $(-(CH_2))$. X. Crystal structure of poly(ethylene oxide). *Macromolecules* **1973**, *6*, 672−675.
(35) Fleer, G. J.; Stuart, M. A. C.; Scheutjens, J. M. H. M.; Cosgrove, T.; Vincent, B. *Polymers at interfaces*; Chapman & Hall: London, 1993.
(36) Lee, H.; de Vries, A. H.; Marrink, S.-J.; Pastor, R. W. A coarse-grained model for polyethylene oxide and polyethylene glycol: conformation and hydrodynamics. *J. Phys. Chem. B* **2009**, *113*, 13186−13194.
(37) Gittings, M. R.; Saville, D. A. Electrophoretic behavior of bare and polymer-coated latices. *Langmuir* **2000**, *16*, 6416−6421.
(38) Hill, R. J.; Saville, D. A.; Russel, W. B. Electrophoresis of spherical polymer-coated colloidal particles. *J. Colloid Interface Sci.* **2003**, *258*, 56−74.
(39) Ottewill, R. H.; Satgurunathan, R. Nonionic latices in aqueous media. Part 2: Stability to added electrolytes. *Colloid Polym. Sci.* **1988**, *266*, 547−553.
(40) Ferrari, R.; Yu, Y.; Lattuada, M.; Storti, G.; Morbidelli, M.; Moscatelli, D. Controlled PEGylation of PLA-based nanoparticles. *Macromol. Chem. Phys.* **2012**, *213*, 2012−2018.
(41) Zackrisson, M.; Stradner, A.; Schurtenberger, P.; Bergenholtz, J. Small-angle neutron scattering on a core-shell colloidal system: a contrast-variation study. *Langmuir* **2005**, *21*, 10835−10845.
(42) Ananthapadmanabhan, K. P.; Goddard, E. D. Aqueous biphase formation in polyethylene oxide - inorganic salt systems. *Langmuir* **1987**, *3*, 25−31.
(43) Israelachvili, J. *Intermolecular & Surface Forces*; Academic Press: San Diego, CA, 1992.
(44) Gaynor, J.; Schueneman, G.; Schuman, P.; Harmon, J. P. Effects of fluorinated substituents on the refractive index and optical radiation resistance of methacrylates. *J. Appl. Polym. Sci.* **1993**, *50*, 1645−1653.